

Supporting Information

Fluorene-Arylamine Copolymers: Separable Control of Hole Transport and Light Emission Through Composition and Conformation

Nikol T. Lambeva, Saurav Limbu, Ji-Seon Kim and Donal D. C. Bradley**

Dr. N. T. Lambeva

Department of Physics, University of Oxford, Parks Road, Oxford OX1 3PU, UK

Present address: Helmholtz-Zentrum Dresden-Rossendorf, Bautzner Landstraße 400, 01328 Dresden, Germany

E-mail: nikol.lambeva@physics.ox.ac.uk; n.lambeva@hzdr.de

Dr. S. Limbu, Prof. J.-S. Kim

Department of Physics and Centre for Processable Electronics, Imperial College London, London SW7 2AZ, United Kingdom

Prof. D. D. C. Bradley

Department of Physics, University of Oxford, Parks Road, Oxford OX1 3PU, UK

NEOM Education, Research, and Innovation Foundation, Al Khuraybah, Tabuk Province, KSA 49643, Saudi Arabia

E-mail: donal.bradley@neom.com

Table of Contents

<i>Section A – Dark Injection Transient Measurements</i>	<i>3</i>
<i>Section B - Copolymer Photoluminescence Spectra</i>	<i>5</i>
<i>Section C – Thermal Treatment Effect on Copolymer Chain Conformation.....</i>	<i>7</i>
<i>Section D – Air Photoemission Spectroscopy.....</i>	<i>12</i>

Section A – Dark Injection Transient Measurements

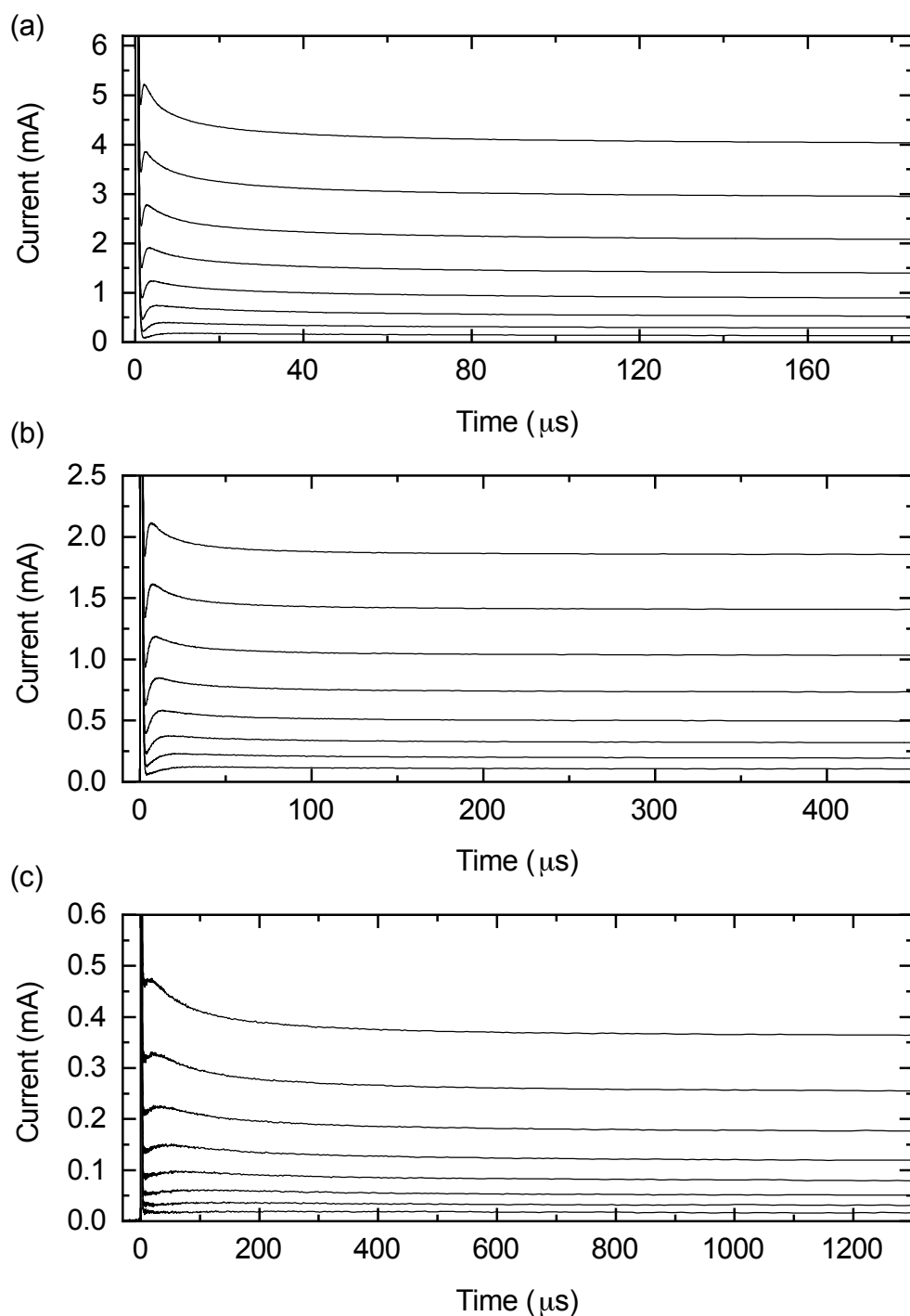


Figure S1. Representative hole injection transients for glassy-phase (a) 280 nm thick film of 80F8:20BSP, (b) 160 nm thick film of 90F8:10BSP and (c) 105 nm thick film of 95F8:5BSP under voltage pulses from bottom to top of 5, 6, 7, 8, 9, 10, 11 and 12 V.

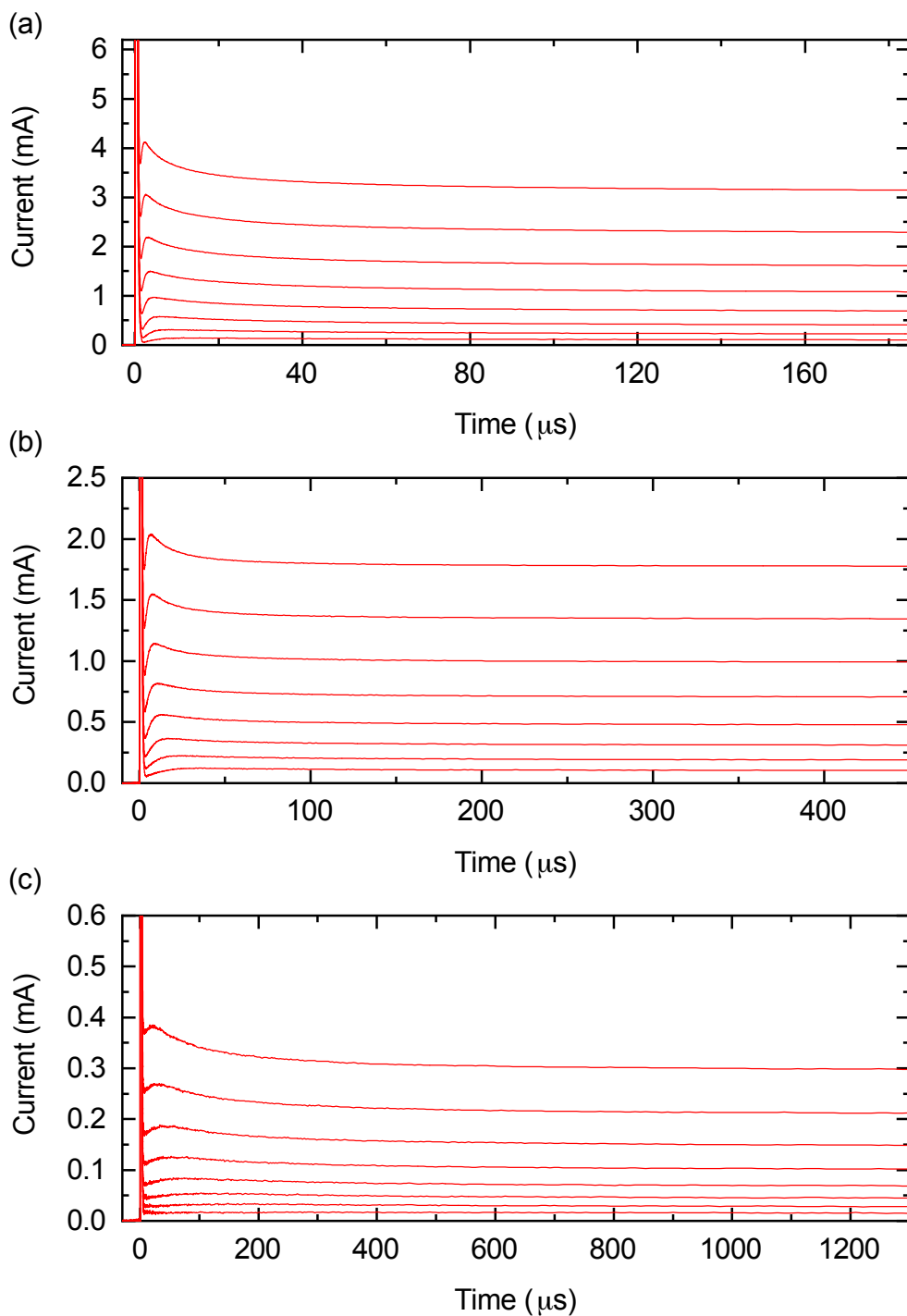


Figure S2. Representative hole injection transients for β -phase (a) 280 nm thick film of 80F8:20BSP, (b) 160 nm thick film of 90F8:10BSP and (c) 105 nm thick film of 95F8:5BSP under voltage pulses from bottom to top of 5, 6, 7, 8, 9, 10, 11 and 12 V.

Section B - Copolymer Photoluminescence Spectra

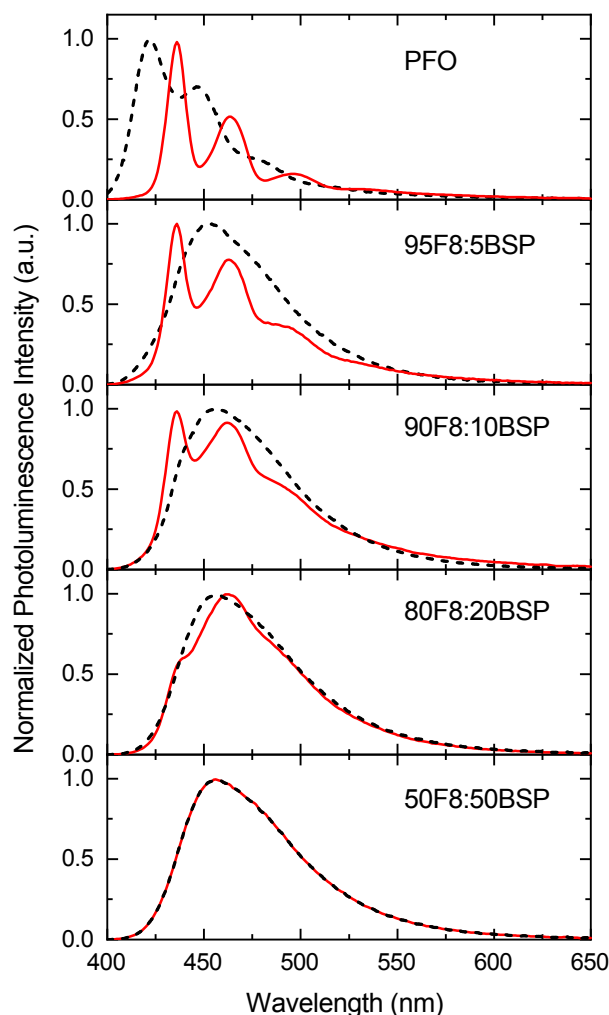


Figure S3. Thin film peak normalized photoluminescence (PL) spectra for hot spun (black dashed line) and solvent vapour treated (red solid line) samples of PFO, 95F8:5BSP, 90F8:10BSP, 80F8:20BSP and 50F8:50BSP.

The hot spin-coated copolymer films show a broad, asymmetric, red-shifted, featureless PL spectrum with a peak at 455 nm. The spectra are very similar to that of the alternating copolymer 50F8:50BSP (PFB). There is no significant PFO emission contribution, therefore suggesting efficient energy transfer from locally excited F8 excitons to BSP-centred excitons.^[1,2] It has been previously shown that the excited states responsible for the copolymer glassy-phase emission have an appreciable charge transfer (CT) character similar to what has been observed for PFB and TFB.^[1,3,4]

The copolymer PL spectra change significantly upon the generation of F8 β -phase chain segments through solvent vapour treatment. The 95F8:5BSP copolymer PL spectrum shows a well-resolved vibronic structure similar to β -phase PFO with the characteristic vibronic peaks at 436, 464 and 498 nm.^[5-8] However, the strength of the S_1-S_0 0-1 and 0-2 vibronic peaks relative to the 0-0 peak is higher for the copolymer compared to PFO. This suggests that the copolymer β -phase PL spectrum is a superposition of β -phase PFO-like structured emission and PFB-like CT emission (**Figure S4**).^[1] Efficient energy transfer from high energy glassy-

phase to low energy β -phase F8 chain segments leads to the dominant β -phase vibronic emission in the spectrum. This is consistent with previous reports of energy transfer between the two phases of PFO.^[5,8] The higher energy β -phase emission component in PL reflects the shorter decay times for β -phase excitons in comparison with the longer-lived CT states.^[1,4] β -phase PL components can also be seen to a lesser extent in the 90F8:10BSP and slightly as shoulders in the 80F8:20BSP copolymer film spectra. This indicates that as the BSP content increases, excitons localize at BSP units preventing migration to β -phase segments, therefore, leading to a stronger residual contribution of BSP-centred emission.

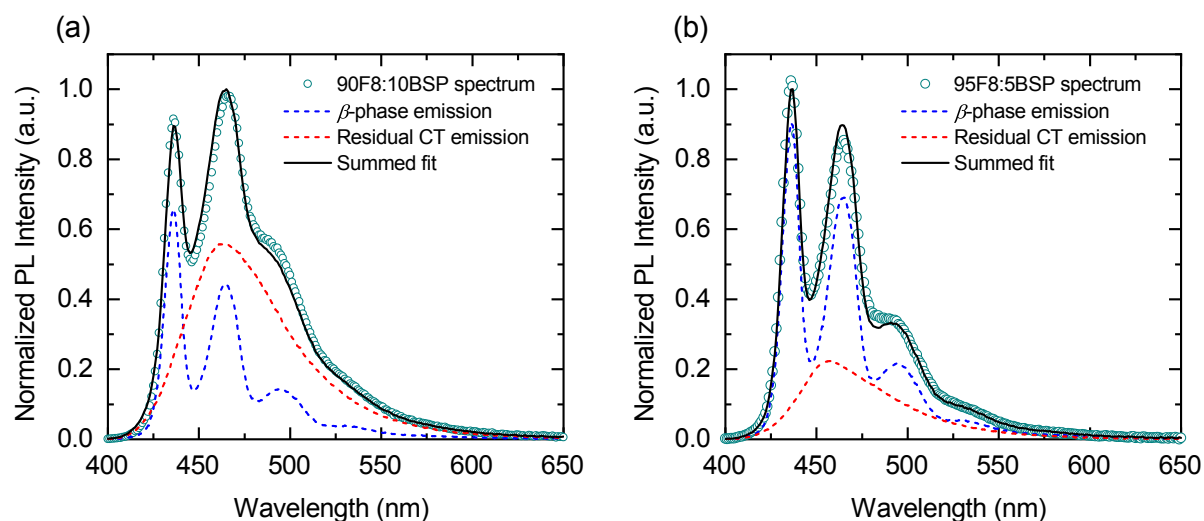


Figure S4. Deconvolution of PL spectra for solvent vapour treated films of (a) 90F8:10BSP and (b) 95F8:5BSP. The dashed red line shows the residual PFB-like CT emission while the dashed blue line displays the vibronic β -phase contribution. The black solid line is the combined sum of both while the open green circles show the experimentally measured PL spectra.

Section C – Thermal Treatment Effect on Copolymer Chain Conformation

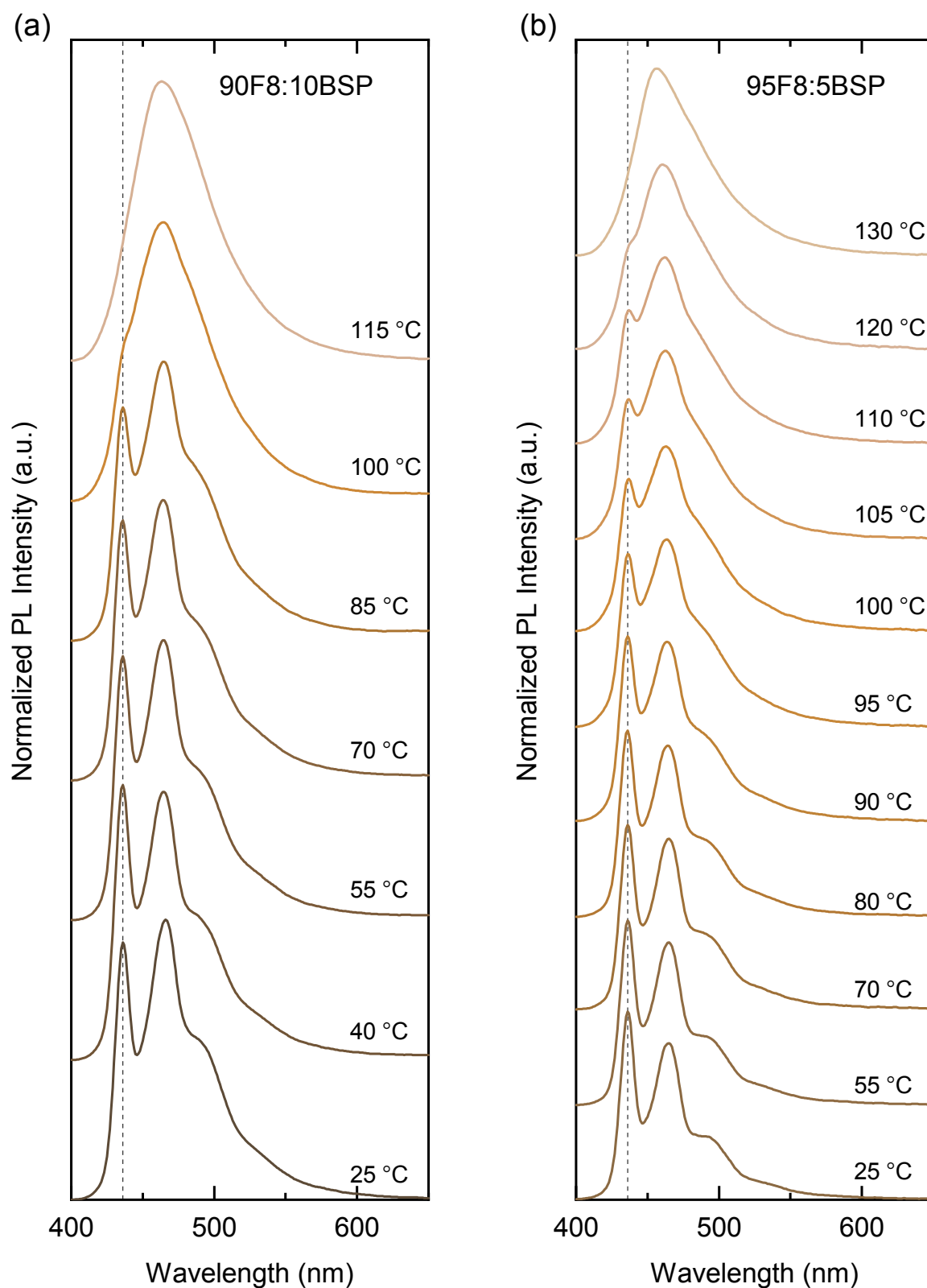


Figure S5. Peak normalized PL spectra for solvent vapour annealed films of (a) 90F8:10BSP following thermal annealing from 25 °C to 115 °C and (b) 95F8:5BSP following thermal annealing from 25 °C to 130 °C. The spectra have been displaced along the vertical axis for ease of comparison. The vertical dashed lines are drawn at the position of the first vibronic peak of β -phase PFO (436 nm).

β -phase 90F8:10BSP and 95F8:5BSP copolymer films were thermally annealed for 10 minutes at stepwise increasing temperatures. The annealing was performed in a nitrogen-filled glovebox to avoid film degradation. After each annealing step the films were allowed to first cool down to room temperature and then the PL spectra and PLQE were measured.

The PL spectra are presented in **Figure S5**. Both copolymer spectra gradually lose their vibronic structure transitioning to the broad, asymmetric glassy phase spectrum above the glass transition temperature T_g .^[9] The increased chain mobility above T_g is effective in disordering the β -phase chain segments. The absence of crystallization for the copolymer films contrasts with reports for PFO,^[10] with the bulky BSP units disrupting close chain packing into an ordered semicrystalline microstructure.

The PLQE values measured for the two copolymer films did not change following thermal annealing. The PLQE of the 95F8:5BSP copolymer had a constant value of $40 \pm 5\%$ while the value for the 90F8:10BSP copolymer was $35 \pm 5\%$. This confirms that the thermal processing did not significantly degrade the emission properties of these materials.

The data was further analysed by deconvolving the spectra to determine the β -phase PL contribution to the emission at each temperature (**Figure S6 and S7**). The PL spectra were fitted to a sum of two reference PL spectra: the PL spectrum of the respective glassy-phase copolymer film (dashed red line) and the PL spectrum of β -phase PFO (dashed blue line). The weightings of the reference spectra were adjusted to sum (solid black line) to the measured PL spectra (open green circles). In the case of the 115°C spectrum for the 90F8:10BSP sample and the 130°C spectrum for the 95F8:5BSP sample the black line is simply the glassy-phase copolymer spectrum as no β -phase PFO component was required for the fit.

The percentage contribution of β -phase emission was then calculated from the ratio of the integrated intensities. This doesn't take account of differences in the respective oscillator strengths and, given the expected larger oscillator strength for β -phase emission, will tend to provide an over-estimate of the β -phase component. The observed small discrepancies between the experimental data and the fits may in part be due to the β -phase PL contribution of the copolymers varying slightly from that for β -phase PFO.

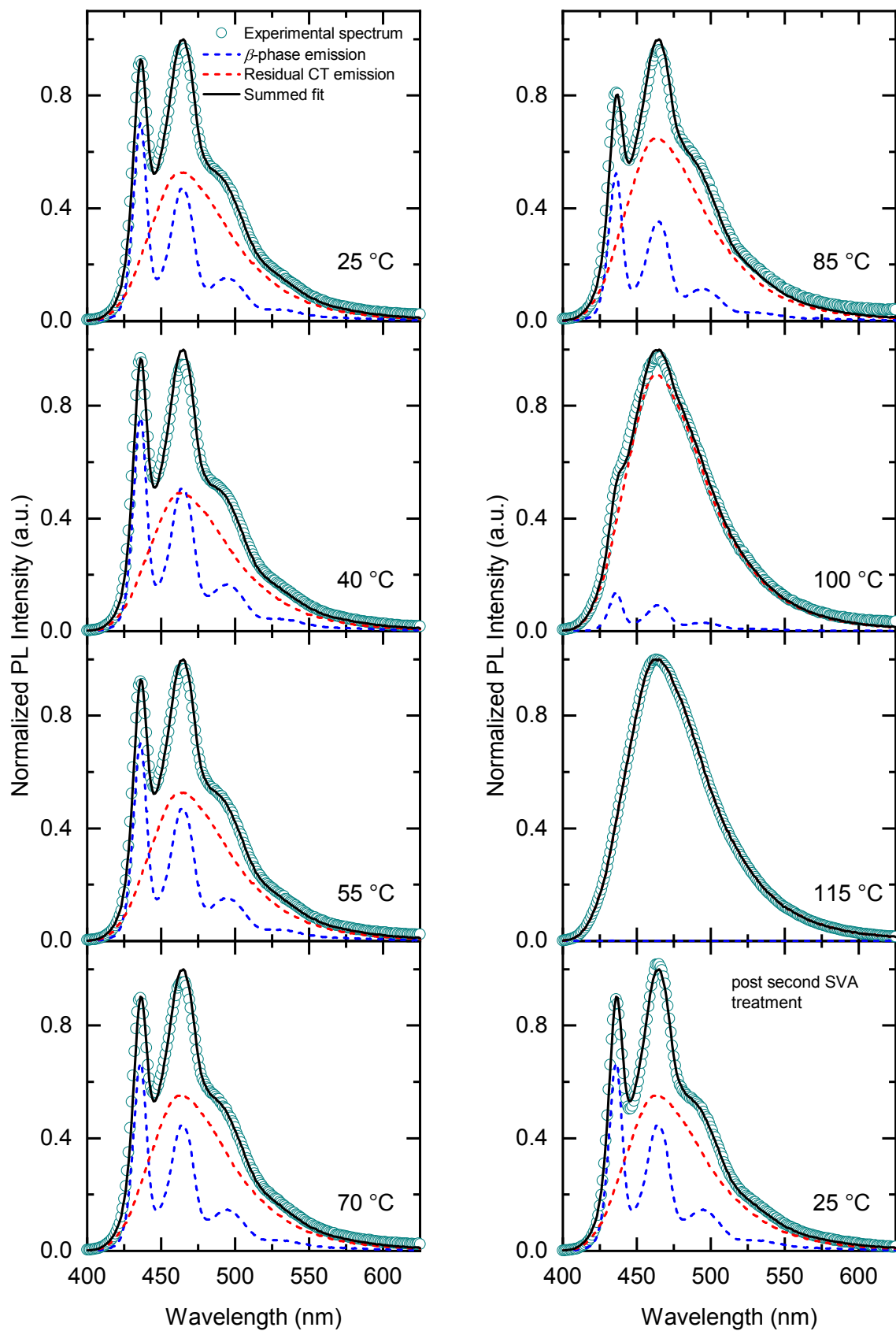


Figure S6. PL spectra and simulated deconvolutions for a 90F8:10BSP solvent vapour annealed (SVA) film before and after thermal annealing for 10 minutes at 40, 55, 70, 85, 100 and 115°C. The spectrum following a second SVA treatment is also presented.

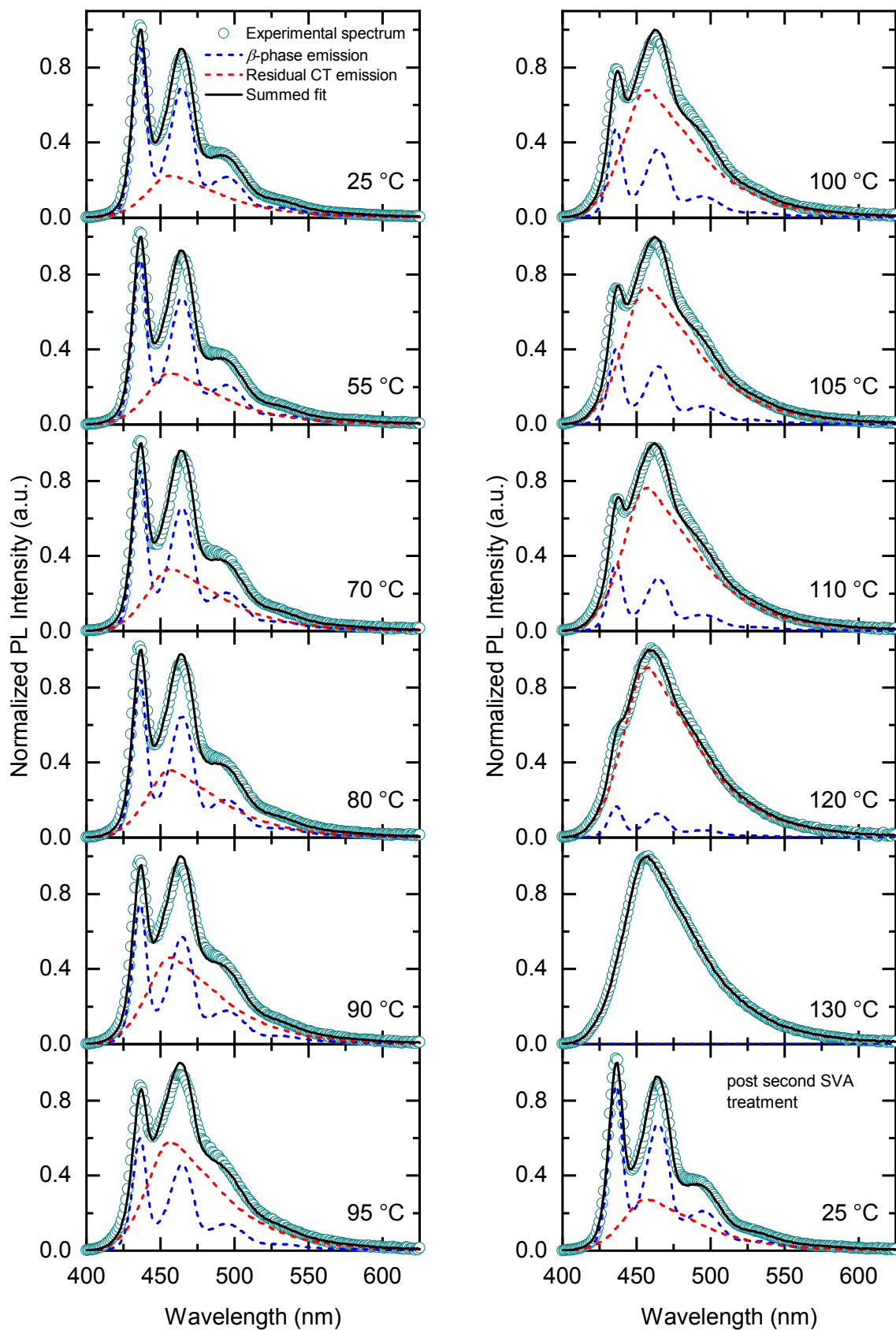


Figure S7. PL spectra and simulated deconvolutions for a 95F8:5BSP SVA film before and after thermal annealing for 10 minutes at 55, 70, 80, 90, 95, 100, 105, 110, 120 and 130°C. The spectrum following a second SVA treatment is also presented.

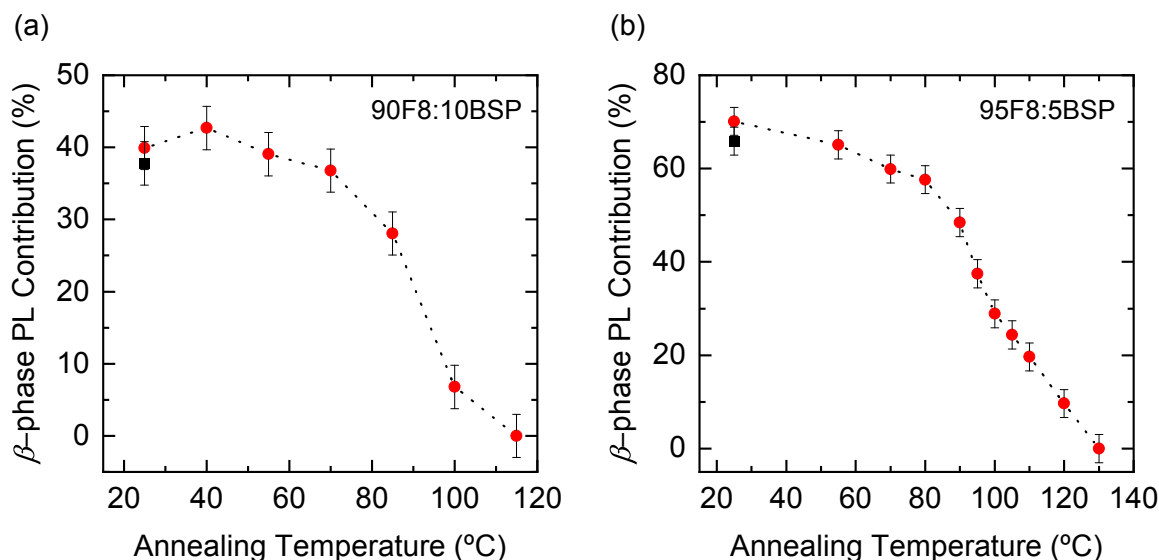


Figure S8. Estimated β -phase contribution to the PL emission spectra as a function of annealing temperature (red circles) for solvent vapour annealed films of (a) 90F8:10BSP and (b) 95F8:5BSP. The β -phase contribution upon a second solvent vapour annealing treatment is shown as a black square for both materials.

As the copolymer films are annealed at higher temperatures their β -phase content is progressively lowered until the films become completely glassy at 100–115 $^{\circ}$ C for 90F8:10BSP and 120–130 $^{\circ}$ C for 95F8:5BSP (**Figure S8**). The difference in the glass transition temperature, T_g , for the two copolymers can be understood on the basis that a higher arylamine concentration will result in more free volume for molecular motion reducing the glass transition for 90F8:10BSP compared to 95F8:5BSP. Upon a second solvent vapour annealing treatment the β -phase conformation was restored in the copolymer films (black squares in **Figure S8**), confirming that these temperature dependent transitions are substantially reversible.

Section D – Air Photoemission Spectroscopy

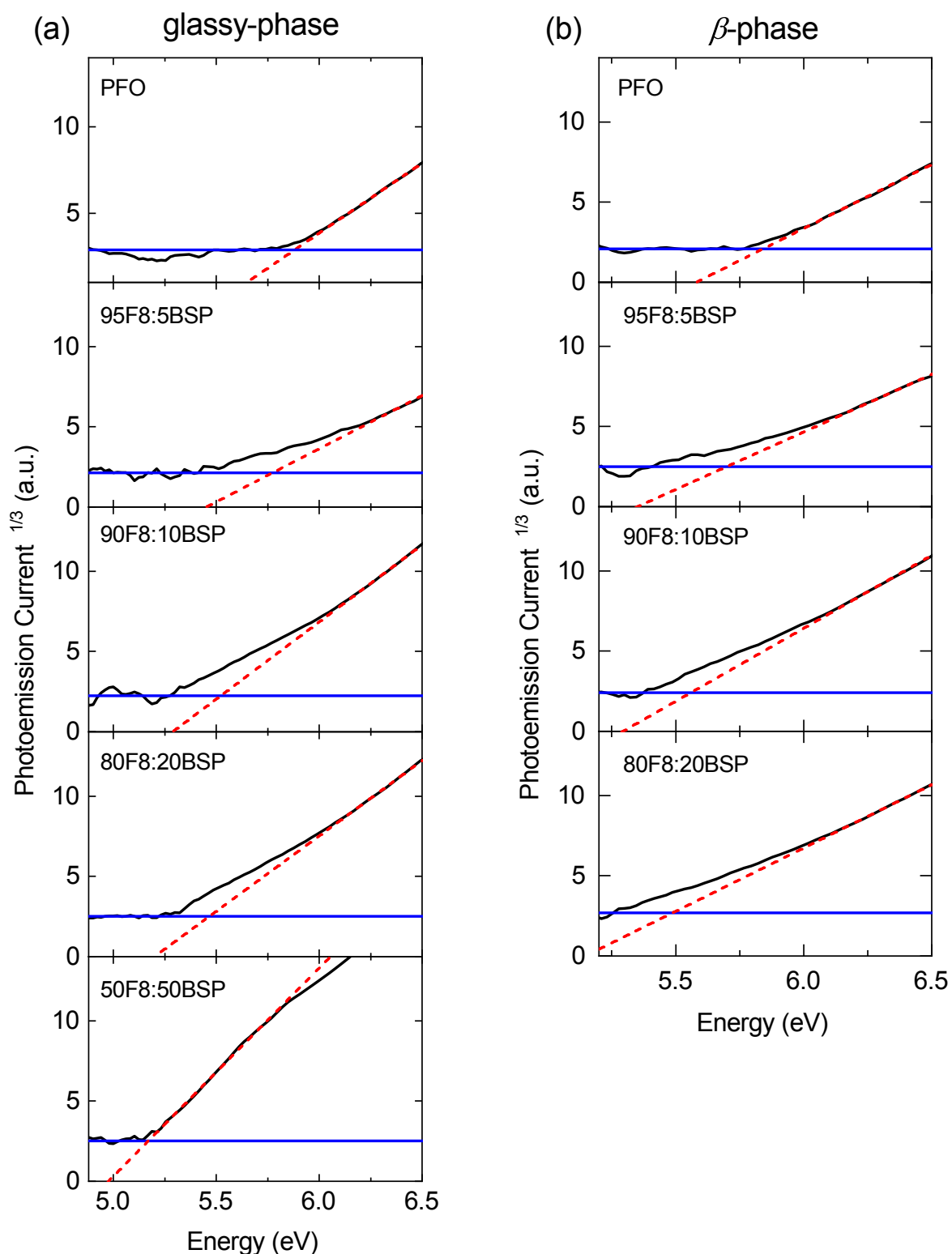


Figure 9. Air photoemission spectroscopy data (black line) for (a) glassy-phase films and (b) β -phase films of PFO, 95F8:5BSP, 90F8:10BSP, 80F8:20BSP and 50F8:50BSP. The energy levels are determined by extrapolating the linear parts of each curve down to their respective baseline signal levels (blue horizontal lines). The dashed red lines are linear fits to the experimental data.

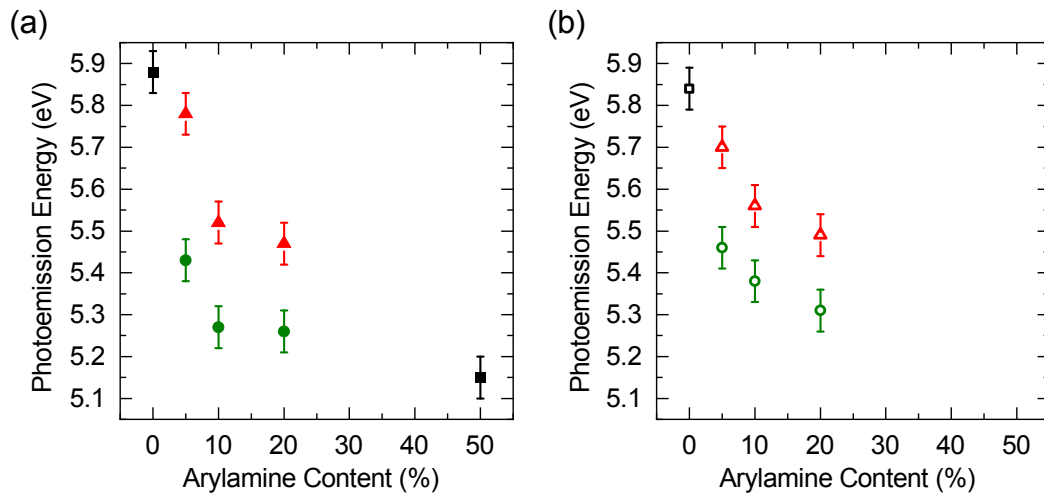


Figure S10. Photoemission energies derived from air photoemission spectroscopy for (a) glassy-phase films (filled symbols) and (b) β -phase films (open symbols) of PFO, 95F8:5BSP, 90F8:10BSP, 80F8:20BSP and 50F8:50BSP. For PFO and 50F8:50BSP a single ionization potential value was extracted (black squares). For 95F8:5BSP, 90F8:10BSP and 80F8:20BSP two distinct contributions are obtained. The lower energy components (photoemission onsets) are denoted by green circles while the higher energy contributions deduced from the red dashed line intercepts in **Figure S9** are represented with red triangles. The addition of only 5% BSP to glassy PFO lowers the APS onset by over 450 meV.

References

- [1] I. Hamilton, N. Chander, N. J. Cheetham, M. Suh, M. Dyson, X. Wang, P. N. Stavrinou, M. Cass, D. D. C. Bradley, J. S. Kim, *ACS Appl. Mater. Interfaces* **2018**, *10*, 11070.
- [2] Y. Tamai, H. Ohkita, H. Benten, S. Ito, *Chem. Mater.* **2014**, *26*, 2733.
- [3] C. E. Richards, R. T. Phillips, *ChemPhysChem* **2011**, *12*, 2831.
- [4] H. Yan, T. W. Tseng, S. Omagari, I. Hamilton, T. Nakamura, M. Vacha, J. S. Kim, *J. Chem. Phys.* **2022**, *156*.
- [5] A. J. Cadby, P. A. Lane, H. Mellor, S. J. Martin, M. Grell, C. Giebeler, D. D. C. Bradley, M. Wohlgenannt, C. An, Z. V. Vardeny, *Phys. Rev. B - Condens. Matter Mater. Phys.* **2000**, *62*, 15604.
- [6] M. Ariu, D. G. Lidzey, M. Sims, A. J. Cadby, P. A. Lane, D. D. C. Bradley, *J. Phys. Condens. Matter* **2002**, *14*, 9975.
- [7] M. Ariu, M. Sims, M. D. Rahn, J. Hill, A. M. Fox, D. G. Lidzey, M. Oda, J. Cabanillas-Gonzalez, D. D. C. Bradley, *Phys. Rev. B - Condens. Matter Mater. Phys.* **2003**, *67*, 1.
- [8] A. L. T. Khan, P. Sreearunothai, L. M. Herz, M. J. Banach, A. Köhler, *Phys. Rev. B - Condens. Matter Mater. Phys.* **2004**, *69*, 1.
- [9] M. Redecker, D. D. C. Bradley, M. Inbasekaran, W. W. Wu, E. P. Woo, *Adv. Mater.* **1999**, *11*, 241.
- [10] M. Sims, K. Zheng, M. C. Quiles, R. Xia, P. N. Stavrinou, D. D. C. Bradley, P. Etchegoin, *J. Phys. Condens. Matter* **2005**, *17*, 6307.